

Application of Response Surface Methodology to Assess the Combined Effect of Operating Variables on the Direct Reduction of Fe_2O_3 by Coal Volatiles

M. Zare ^{1*}, J.Vahdati-Khaki ², A. Zabet ³

Department of Materials Engineering, Faculty of Engineering, Ferdowsi University of Mashhad, Mashhad, Iran.

Abstract

The reduction of Fe_2O_3 powder at the top layer by the volatiles from high volatile (HV) bituminous coal at the bottom layer of a multilayer powder geometry including a separating alumina layer was studied. The simultaneous effects of the alumina layer thickness, time, temperature and the weight of coal on the amount of reduction and coal devolatilization were studied by implementing a rotatable central composite design (CCD) based on response surface methodology (RSM). RSM successfully revealed the influential operating variables and the effects of the interactions between the variables on the reduction of Fe_2O_3 and devolatilization of coal. The phase evaluation of various iron oxide phases and metallic iron was obtained through XRD. The XRD results showed that the reduction of pure Fe_2O_3 to metallic iron proceeded through a stepwise reduction via Fe_3O_4 and FeO. It was also found that the reduction of iron oxide by coal volatiles occurred internally uniformly at the first stage of reduction to form Fe_3O_4 ; however, the behavior became nearly topochemical as the reduction proceeded.

Keywords: Coal volatile; Iron oxide reduction; Response surface methodology; Analysis of variance.

1. Introduction

Various features of non-coking coal-based direct reduction processes have been investigated in the literature^{1,2}. Many works have been focused on the process conditions test, energy saving and reducing consumption. Some researchers have studied incorporating non-reacting volatiles in the course of reduction^{3,4}.

Non-reacting volatiles evolved without any contribution to the overall reductions have been a debatable issue for the investigators. Depending upon the final temperature and the heating rate, large amounts of volatile matter ranging from light gases, such as CO , CO_2 , H_2 , CH_4 , to heavy hydrocarbons, such as C_nH_m , may be evolved from the non-coking coal in which CO and H_2 are found to be reducing gases⁵.⁶ Some investigations have been carried out to demonstrate the possibility of implementing coal volatiles in a multi-layer reduction process by which the volatile matter can contribute direct reduction reactions³.⁷ This concept is based on the consideration that the volatile stream from bottom layers can be involved in direct reduction by passing through the upper iron oxide layer as the reducing matter. In such as condition,

volatile matter will not actively react with the Fe_2O_3 layers until they adequately remain in contact with iron oxide particles^{2,7}.

Processing factors such as temperature, time and coal amount can affect the percentage of reduction and coal devolatilization, and their effects may be either independent or interactive. In a novel system including Fe_2O_3 powder at the top layer, bituminous coal at the bottom and a separating alumina layer of multi-layer powder geometry, the thickness of alumina layer (ALT) can be considered as a variable. It should be mentioned that the effect of this factor on the reduction should be determined in separate experiments, but the interactive effect of ALT alongside with temperature, time and coal amount can be investigated by response surface methodology.

Response surface methodology (RSM) using a sequence of designed experiments defines the effect of the independent variables, alone or in combination, on the processes⁸. The RSM is utilized as a statistical design to establish the relationships between the response and operating variables in complex processes such as nano-particle milling process⁹, thermal barrier coating using plasma spraying⁹, corrosion of titanium alloys¹⁰, welding¹¹, modeling of iron ore pelletization¹² and high pressure coal gasification process¹³.

However, there have been few works on the adaptation of statistical design of experiments, including RSM, in the direct reduction of iron. Dai et al. adapted RSM to optimize the process variables for

* Corresponding author:

Tel: +98 936 4479786

E-mail: Mansoor.zare18@gmail.com

Address: Department of Materials Engineering, Faculty of Engineering, Ferdowsi University of Mashhad, Mashhad, Iran.

1. M.Sc.

2. Professor

3. Assistant Professor

reduction of iron by microwave heating¹⁴. The influence of ore particle size, coal particle size, coal/ore ratio, time and temperature on the direct reduction of a column of iron ore fines surrounded by coal fines was studied using the design of experiment¹⁵. They found the interaction between the main processing variables important in the reduction rate of iron ores.

In the present investigation, the combined effects of the operating variables, namely, temperature, time, coal amount and alumina layer thickness (ALT), on the percentage of reduction and coal devolatilization were studied using response surface methodology (RSM). The reduction course of initial Fe_2O_3 by coal volatile was also investigated using X-ray diffraction (XRD) analysis.

2. Materials and Experimental Procedures

2.1. Sample chemistry

High purity iron oxide powder was purchased from Loba Chemie Co. (India) with the chemical composition and particle size listed in Table 1. The chemical analysis of hematite was done using X-Ray Fluorescence (XRF) analysis. For devolatilization purpose, a high volatile bituminous coal from Gol-Banoo mine was used. Proximate analysis and particle size of the coal are given in Table 2. Alumina powders with a particle size smaller than $50\ \mu m$ (#-270) were also purchased in commercial composition.

Table 1. Size distribution and chemical composition of Hematite samples by X-Ray Fluorescence (XRF)

Item	SiO ₂	Al ₂ O ₃	TiO ₂	MnO	CaO	P ₂ O ₅	Fe	size
Wt.(%)	0.01	0.03	0.02	0.21	0.05	0.05	69.17	-270#

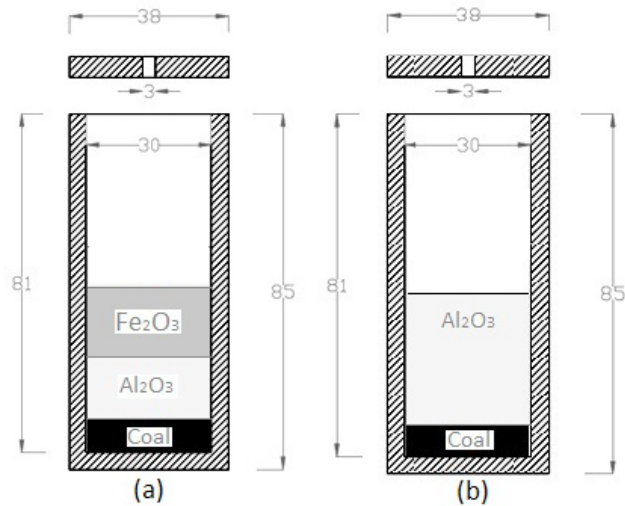
Table 2. Size distribution and proximate analysis of coal

Item	Moisture	Ash	V.M.	F.C.	size
Wt.(%)	2	8	38	52	-200#

2.2. Multilayer iron oxide reduction system

It is important to distinguish the sole effect of volatiles on the degree of reduction. Figure 1 shows a schematic of the method used for achieving this goal. As can be seen, two stainless steel crucibles were used, one as the main container and the other as the representative crucible. The main crucible (A) contained 3 layers of coal, alumina and iron oxide and the representative crucible (B) had layers of coal and alumina powder. The crucibles were both threaded in one end so that they could be closed with the holed caps for the free release of the gases. Before each experiment, the powders (coal, Fe_2O_3 , and Al_2O_3) were dried for one hour at $110^\circ C$. Then, the dried powders were poured into the cylindrical crucibles with no compaction. The

loaded crucibles were heated in a muffle furnace at the heating rate of $12^\circ C/min$ until the furnace temperature reached the assumed temperature (which was selected to be 700, 800 and $900^\circ C$) and then they were kept isothermally. After a predetermined time, the crucibles were taken out of the furnace and cooled. During cooling, the caps holes were sealed to prevent the re-oxidation of reduced iron oxide.



Note: All the units are in mm.

Fig. 1. Vertical cross section of reaction crucibles: (a) the main sample and (b) the representative sample.

2.3. Determination of iron oxide reduction

In each experiment, the sole effect of volatile evolution was obtained from the weight loss associated with crucible (B). On the other hand, the weight loss with crucible (A) was due to the volatile evolution and the reduction of the Fe_2O_3 layer. Therefore, the sole effect of Fe_2O_3 reduction by volatile was determined by subtracting the weight loss of reactors A and B. The degree of devolatilization and the degree of reduction (%) were then calculated using the following formula:

$$\% \text{ Devolatilization} = \frac{\Delta W_{(Coal)}}{W_{(Coal)}} \times 100 \quad (1)$$

$$\% \text{ Reduction} = \frac{\Delta W(Fe_2O_3)}{W(O_2)} \quad (2)$$

such that

$$W(O_2) = \eta_{Fe_2O_3} (48/160) W_{Fe_2O_3} \quad (3)$$

The term $\eta_{Fe_2O_3}$ represented the purity of Fe_2O_3 in the initial iron oxide; $W(Fe_2O_3)$ and $W(Coal)$ denoted the weight of iron oxide and the weight of coal, respectively; $\Delta W(Coal)$ was the weight loss with crucible (A) and $\Delta W(Fe_2O_3)$ was calculated from subtracting weight loss with crucibles A and B.

3. Design of Experiments

3.1. The experimental design

Several experimental studies have been conducted to choose the central composite design (CCD) as an efficient technique to establish the equation of response surface¹⁶. This procedure creates designs with desirable statistical properties, but with only a fraction of the whole required experiments. With four variables each in five levels, the design is composed of a total 30 experiments (design points) containing 16 factorial points, 8 axial points and six replicates at the center point of the design. To simplify the calculations, the independent variables are normally coded to (-1, 1) interval according to the equation coming below,

$$X_i = (x_i - x_i^0) / \Delta x_i \quad (4)$$

where X_i denotes the coded value, x_i is the actual value of the i^{th} variable and Δ_{x_i} is the step size. x_i^0 represents the value of x_i at the so-called center point of the inspected area. The real and coded values for each parameter and the range of parameters applied for the experiments are given in Table 3. Based on some preliminary experiments, the levels of the variables were chosen. As the volatiles were released, in order to prevent the powders from agitation, ALT was selected such that the maximum bed height was maintained around 40 mm. The coal weight in the middle level (level zero) was chosen based on the stoichiometric requirement for reduction by the following reaction:



Table 3. Actual and coded values of the operating variables.

Independent variable	Factor	levels					
		X_i	$(-1.414)-\alpha^a$	-1	0	1	$+\alpha(+1.414)$
A: temperature (°C)	x_1		660	700	800	900	940
B: time (min)	x_2		6	15	37	60	70
C: Coal weight	x_3		2.76	2.90	3.25	3.60	3.75
D: ALT ^b (mm)	x_4		14	20	35	50	56

^a α the position of the axial point of the cubic

^b ALT: Al_2O_3 bed thickness

The central composite design is shown in Table 4. As can be seen, each row represents individual experiment and the columns denote the associated factors. The last columns of the table correspond to the responses of the design, which are reduction and devolatilization percentage.

Table 4. Experimented conditions in a coded form corresponding to the design variables and the responses.

Run no.	Point type	X_1	X_2	X_3	X_4	Reduction (%)	Devolatilization (%)
1	Factorial	-1	-1	-1	-1	6.8	25.9
2	Factorial	+1	-1	-1	-1	30.1	43.3
3	Factorial	-1	+1	-1	-1	7	30.9
4	Factorial	+1	+1	-1	-1	25.2	46.6
5	Factorial	+1	-1	+1	+1	8.3	23.9
6	Factorial	+1	-1	+1	-1	35.3	41.3
7	Factorial	-1	+1	+1	-1	7.2	29.7
8	Factorial	+1	+1	+1	-1	32.1	43.9
9	Factorial	-1	-1	-1	+1	7	23.1
10	Factorial	+1	-1	-1	+1	31.2	44.9
11	Factorial	-1	+1	-1	+1	8.1	31.3
12	Factorial	+1	+1	-1	+1	26.9	44.9
13	Factorial	-1	-1	+1	+1	8.4	21.7
14	Factorial	+1	-1	+1	+1	36.7	39.1
15	Factorial	-1	+1	+1	+1	8.7	27
16	Factorial	+1	+1	+1	+1	32.7	42.8
17	Axial	$-\alpha$	0	0	0	3.7	18.8
18	Axial	$+\alpha$	0	0	0	42.1	45.3
19	Axial	0	$-\alpha$	0	0	14.7	35.8
20	Axial	0	$+\alpha$	0	0	16.2	41.0
21	Axial	0	0	$-\alpha$	0	15.2	41.6
22	Axial	0	0	$+\alpha$	0	20.1	35.1
23	Axial	0	0	0	$-\alpha$	19.9	38.3
24	Axial	0	0	0	$+\alpha$	16.2	40.7
25	Center	0	0	0	0	20.1	37.5
26	Center	0	0	0	0	20	39.1
27	Center	0	0	0	0	19.9	38.2
28	Center	0	0	0	0	18.8	39.5
29	Center	0	0	0	0	20.9	38.4
30	Center	0	0	0	0	20.8	39.3

3.2. Response surface modeling

RSM is an experimental strategy for exploring the space of the process independent variables. Empirical statistical modeling is used to develop an appropriate relationship between the yield and the process variables, and optimization methods are employed for finding the levels or values of the process variables that produce the desirable values of the responses⁸. In general, the relation between response variable Y , which depends upon the k process independent variables X_1, X_2, \dots, X_k , can be expressed as:

$$y = f(x_1, x_2, \dots, x_k) + \varepsilon \quad (6)$$

where x_1, x_2, \dots, x_k are the respective values of the independent variables X_1, X_2, \dots, X_k , and ε represents the noise or error observed in the response y , which is assumed to follow a normal distribution with mean zero and variance σ^2 across all values of Y . If we denote the expected response by $E(Y) = f(X_1, X_2, \dots, X_k) = \eta$, then the surface represented by $\eta = f(X_1, X_2, \dots, X_k)$ is called a response surface.

Usually, a low order polynomial is employed in RSM models¹⁷⁾. However, direct reduction processes are often considered to possess a nonlinear relationship between the input of the system and the output response yield. So first order models may not be adequate here. In addition, second-order models may better account for the interactions among independent variables; hence they are more appropriate than the first-order models. Consequently, the second-order model was employed in this study and the proposed response equation was presented as follows:

$$y = \beta_0 + \sum_{i=1}^k \beta_i x_i + \sum_{i=1}^k \beta_{ii} x_i^2 + \sum_{i < j} \beta_{ij} x_i x_j + \varepsilon \quad (7)$$

where β_0 , β_i , β_{ii} and β_{ij} are coefficients for the corresponding terms, and ε is the random error.

4. Results and Discussion

4.1. Analysis of variance (ANOVA) for finding the RSM order

The ANOVA results for fitting the linear, interactive, quadratic and cubic terms to the data obtained from experiments are given in Table 5. By considering the significant level of 0.05 ($\alpha=0.05$), the ‘Lack of Fit p-value’ for either the reduction or devolatilization implies that the lack of Fit’s is significant relative to the pure error using only linear terms. The table also indicates that the contribution of the corresponding quadratic terms to Eq. (3) is significant and it should be considered in the final regression models.

Table 5. Analysis of variance for finding the regression order.

Source	Reduction (%)			Devolatilization (%)		
	Sequential p-value	Lack of Fit p-value	Adjusted R-Squared	Sequential p-value	Lack of Fit p-value	Adjusted R-Squared
Linear	0.0001	0.0065	0.9379	<0.0001	0.0006	0.8875
Intraction ^a	0.2671	0.0072	0.9502	0.8971	0.0003	0.7837
Quadratic	0.0028	0.0385	0.9521	<0.0001	0.0414	0.9500
Cubic	0.2823	0.0275	0.6590	0.2861	0.0294	0.4908

4.2. ANOVA for fitting RSM

ANOVA analysis was established in order to evaluate the influential factors in the quadratic RSM. The ANOVA results for the quadratic model of the degree of reduction (% R) are presented in Table 6. The model “P-value” of 215.10 indicated that the there was only a 0.01% chance that a “Model F-value” of this size could occur due to noise. From the table, all linear terms, the interaction terms of X_1X_2 , X_1X_3 and quadratic terms of x_1^2 and x_2^2 were found to have significant effects on the reduction by volatile.

The ANOVA results for the quadratic model of the degree of coal devolatilization (% Dev) are presented in Table 7.

The model “F-value” of 263.35 also implied that the response quadratic model was highly significant. Based on the consideration that the factor a “P-value” less than 0.05 is a significant term, the linear terms of X_1 , X_2 , X_3 , X_4 , the interaction term of X_1X_2 and the quadratic term of X_1^2 could be significant model terms for the degree of coal devolatilization. Finally, the assumptions for randomness, normality and constant variances of the residuals were all checked and verified by diagnostic plots including the normal probability plot and the residual plot.

Table 6. Significance of RSM model and variables using ANOVA analysis for the degree of iron reduction.

Source	Some of Squares	DOF ^a	F-Value	P-vale Prob>F
Model	3114.348	8	215.104	<0.0001
X_1	2942.778	1	1626.031	<0.0001
X_2	9.02434	1	4.986397	0.0366
X_3	56.58129	1	31.26398	<0.0001
X_4	9.000435	1	4.973188	0.0368
$X_1 \times X_2$	17.28481	1	9.550715	0.0055
$X_1 \times X_3$	23.44981	1	12.95718	0.0017
X_1^2	38.8977	1	21.49291	0.0001
X_2^2	31.2494	1	17.26685	0.0004
Residual	38.00563	21		

Table 7. Significance of RSM model and variables using ANOVA analysis for the degree of coal devolatilization.

Source	Some of Squares	DOF	F-Value	P-vale Prob>F
Model	1751.045	7	263.3524	<0.0001
X_1	1458.063	1	1535.021	<0.0001
X_2	85.05301	1	89.54219	<0.0001
X_3	47.13183	1	49.6195	<0.0001
X_4	9.918111	1	10.4416	0.0038
$X_1 \times X_2$	13.48726	1	14.19913	0.0011
X_1^2	136.5413	1	143.748	<0.0001
Residual	20.89703	22		

Therefore, it can be concluded that the quadratic model could be adequate to describe both response surface models. ‘Design expert-8’ software was employed to fit the data to the response surfaces and the final equations in terms of the coded values were obtained as follows:

$$\%R = 19.2 + 12.13 X_1 - 0.67 X_2 + 1.68 X_3 + 0.67 X_4 - 1.04 X_1 X_2 + 1.21 X_1 X_3 + 1.97 X_1^2 - 1.77 X_2^2 \quad (8)$$

$$\%Dev = 38.72 + 8.54 X_1 + 2.06 X_2 - 1.54 X_3 - 0.70 X_4 - 0.92 X_1 X_2 - 3.58 X_1^2 \quad (9)$$

By comparing the coefficients of the term X_4 , it could be seen that alumina layer had a positive effect on the

degree of reduction while the degree of coal devolatilization was decreased simultaneously. This proved that the alumina layer significantly affected the reduction of iron oxides. It is more likely that the alumina layer delayed volatiles to release until the temperature of iron oxide was adequately increased for reacting with the reducing agents of volatiles. Other terms having combined effects on the responses are discussed later.

4.3. Interpretation of RSM plots

To elucidate the effects of the operating variables on the responses, their relationship has been showed graphically. The plots were generated based on equations 6 and 7 as a function of employing a pair of significant variables and holding other variables at their zero levels.

Fig. 2 (a, b) shows the response surface plots for the degree of reduction and coal devolatilization with respect to time and temperature when coal weight and ALT were fixed at their middle values (3.25 g and 35 mm). As can be seen from Fig. 2 (a), the degree of reduction was increased with the increase in temperature. On the other hand, the penetration of oxygen to the reduced iron, due to decreasing the outflow of volatiles and its subsequent reduction potential, oxidized the reduced samples at the prolonged time. Fig. 2 (b) indicates that coal devolatilization was increased as temperature was raised. This was expected given that devolatilization of coal was a thermally activated process.

Fig. 2 (c, d) shows the response surface plots for the degree of reduction and coal devolatilization with respect to coal weight and temperature when time and ALT were fixed at their middle values (37 min and 35 mm). From Fig. 2 (c), the degree of reduction was increased as the amount of coal was increased; however, at lower temperatures, the effect was not appreciable. As the weight of coal was increased, the total volatile matter evolved from coal was increased. From the plots, for instance, at 900 °C, the total volatile for 2.9g, 3.25 g and 3.6 g was found to be 1.39g, 1.43g and 1.50 g, respectively. The greater amount of volatiles served more as reducing agents (CO and H₂) in reaction sites which could potentially reduce the iron oxides.

However, the reduction reactions could be kinetically improved by increasing the temperature. On the other hand, CH₄ and other hydrocarbons such as C_nH_m could be cracked to C and H₂ at temperatures higher than 550°C, reducing the oxides directly; however, the kinetics of C_nH_m cracking as elemental C and H₂ at low temperatures was too slow for any effective reduction¹⁸). The cracking of C_nH_m is presented be



Fig. 2 (d) shows that the devolatilization degree (total volatile evolved per gram of coal) was decreased with the weight of coal. It seemed that the greater height of coal bed resulting from the greater weight of coal delayed the escape of volatiles from the crucible.

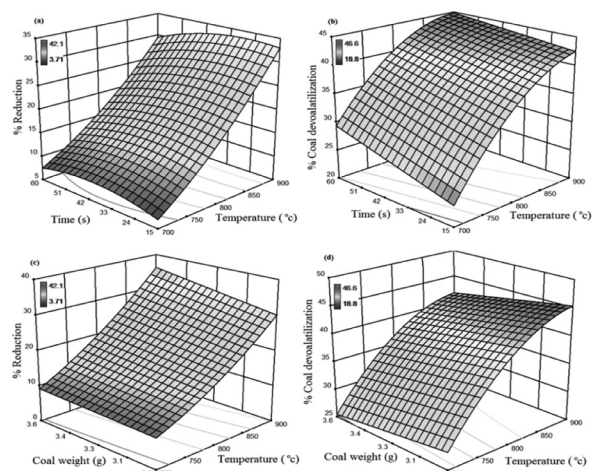


Fig. 2. Response surface plots representing the combined effect of time-temperature on the degree of reduction (a), coal devolatilization (b), the combined effect of coal weight-temperature on the degree of reduction (c) and on coal devolatilization (d).

4.4. Verification experiments

Fig.3 shows the predicted values versus the experimental results used to obtain the models (O). The figure clearly shows that there was a good correlation between both values as substantiated by the coefficient of determination R² (%Reduction, %Devolatilization) = (0.9986, 0.9992). Five additional experiments employed to cover the entire experimental range of the study were carried out in order to check the adequacy of the developed models for the response variables studied. The experimental conditions for verification experiments are given in Table 8. Figure 3 also shows that the verification values (Δ) fell very closely on the regression line, thereby indicating the robustness of the models. Thus, it indicated that the proposed quadratic polynomial equations could describe adequately the influence of the selected independent variables (temperature, time, coal weight and ALT) on the responses studied during the direct reduction of hematite by volatiles.

Table 8. Verification experiments outside the designed experiments for checking the adequacy of the RSM model.

Test	A	B	C	D	%Reduction		%Devolatilization	
	°C	min	g	mm	Exp. ^a	Pred. ^b	Exp.	Pred.
a	700	40	3.25	48	7.8	9.4	32.9	31.3
b	750	38	3.25	48	15.7	15.1	23.8	23.1
c	800	34	3.6	45	23.1	21.8	39.1	36.5
d	850	31	3.6	50	28.6	29.3	38.4	39.7
e	900	29	3.6	45	38.5	37.6	40.2	41.2

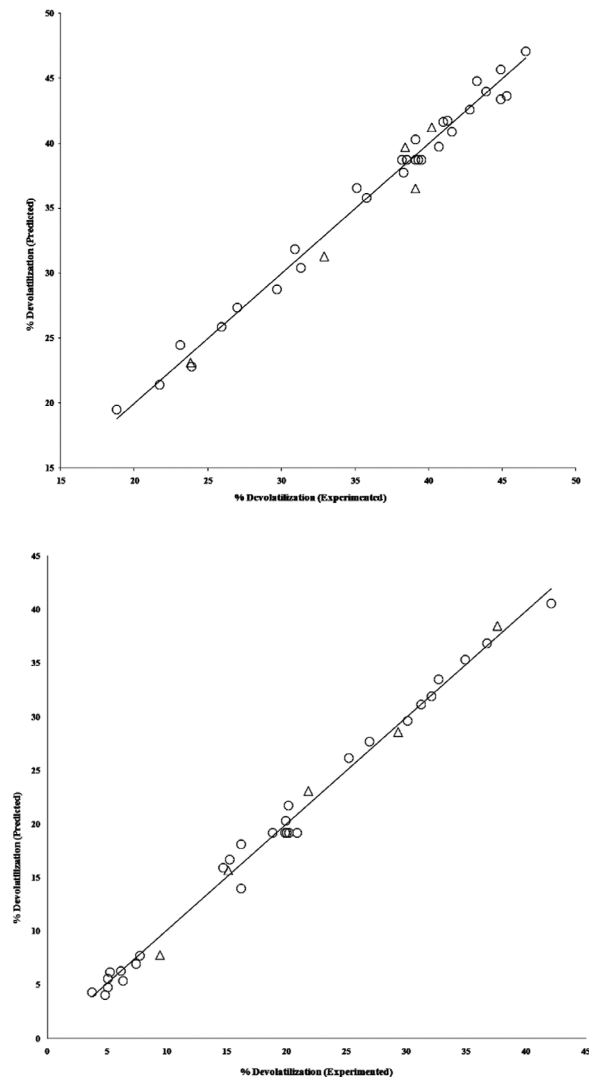


Fig. 3. Theoretical values of the response variables predicted from the respective models versus the experimental values. (o): Experiments used for the calculations of the models. (Δ): Additional experiments not forming part of the experimental design

4.5. X-ray diffraction analysis

Three samples from the partially reduced iron oxide at different amounts of reduction were chosen for XRD analysis. Fig. 4 illustrates the XRD pattern of the samples. The sample (a) with 7.8% reduction showed the partial reduction of Fe_2O_3 to Fe_3O_4 . The appearance of FeO was obvious in the sample (b) with 12.7%, while the initial Fe_2O_3 was no longer seen, thereby indicating that the first step reduction of Fe_2O_3 forming Fe_3O_4 was initiated below 7.8 pct reduction and completed below 12.7 pct of reduction. On the other hand, the second step reduction of Fe_3O_4 to form FeO was initiated below 12.7 pct and completed below 38.5 pct reduction, since there was no sign of Fe_3O_4 in sample (d) with 38.5pct reduction. XRD pattern of the sample (c) indicated that the third step reduction of FeO to form metallic Fe was initiated below 35 pct reduction as the metallic phase of Fe could be seen in the sample.

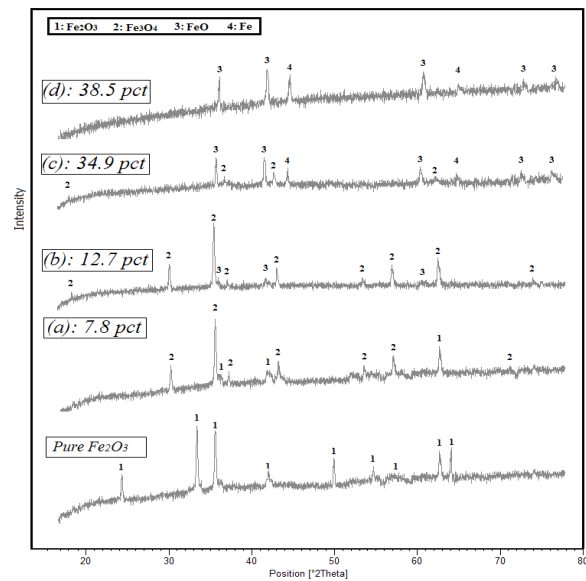
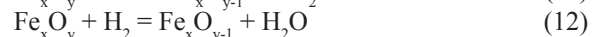


Fig. 4. X-ray diffraction analysis of reduced iron ores at different amounts of reduction by coal volatiles.

According to XRD results, the Fe_2O_3 underwent stepwise reductions by CO and H_2 , which could be represented by the following reactions¹⁹⁻²¹:



where, x and y represent the molar fractions of Fe and O, respectively. Based on the above reactions, Fe_2O_3 was reduced to Fe_3O_4 at the first stage of reduction, followed by the subsequent reduction of Fe_3O_4 to FeO and FeO to the metallic iron. Owing to the stoichiometry of the stepwise reaction of hematite to metallic iron, transformation of Fe_2O_3 to Fe_3O_4 , Fe_3O_4 to FeO and FeO to metallic iron was completed around 11%, 33% and 67%, respectively. This was contingent upon the condition that the reduction could take place uniformly through the samples²². For the sample (a), the fraction reduced corresponded to 12.7 pct, which was close to the reduction to Fe_3O_4 by assuming a uniform internal reduction. This coincided with the results found for the first step reduction of highly porous powders of hematite (PAH) to Fe_3O_4 ²³.

However, the fraction reduced corresponded to 35.9 pct at the sample (c) and did not fit the aforementioned assumption, thereby indicating that the behavior became nearly topochemical as the reduction proceeded. This suggested that the reduction of porous iron oxide bed by coal volatiles occurred internally uniformly at the first stage of reduction; however, the degree of uniform reduction was decreased with increasing the reduction percentage.

5. Conclusions

This study was set out to apply response surface methodology to approach the reduction of Fe_2O_3 by coal volatiles in a multilayer iron reduction system.

The following conclusions can be drawn from experimental results based on the strategy employed:

1. The proposed quadratic models could suitably assess the amount of Fe_2O_3 reduction and coal devolatilization at any area of the experimental domain. Coefficient of determination (R^2) calculated for both models exceeded 0.99, thereby showing good correlations between the predicted values versus the experimental results.

2. Other than the linear terms of temperature, time, coal weight and thickness of alumina bed, the simultaneous effects of time-temperature and coal weight-temperature influenced the reduction of iron oxide by volatile. Also, the aforementioned linear terms, along with the interaction between time and temperature, were significant parameters affecting the devolatilization of coal. The most significant variable affecting the amount of iron reduction and coal devolatilization was also found to be temperature.

3. The initial Fe_2O_3 underwent a three-step stepwise reduction to form metallic irons and occurred through a uniform internal reduction during the first step reduction of hematite to form Fe_3O_4 . As reduction proceeded, it became topochemical across the partially reduced iron oxide bed.

Abbreviations

HV	high volatile
CCD	central composite design
ALT	Al_2O_3 layer thickness
XRD	X-ray diffraction
EDS	energy dispersive X-ray spectroscopy
RSM	response surface method
ANOVA	analysis of variance

References

[1] T. Sharma, *Int. J. Miner. Process.*, 39 (1993), 299.
 [2] S.K. Dutta, A. Ghosh, *Metall. Mater. Trans. B*, 25 (1994), 15.
 [3] I. Sohn, R.J. Fruehan, *Metall. Mater. Trans. B*, 37 (2006), 231.
 [4] H. Konishi, K. Ichikawa, T. Usui, *ISIJ Int.*, 50 (2012), 386.

[5] R.S. Sampaio, *Coal Devolatilization in Bath Smelting Slags*, Carnegie Mellon University, Pittsburgh, (1990), 26.
 [6] J.G. Speight, *The chemistry and technology of coal*, M. Dekker, (1994), 392.
 [7] I. Sohn, R.J. Fruehan, *Metall. Mater. Trans. B*, 37 (2006), 223.
 [8] R.H. Myers, D.C. Montgomery, C.M. Anderson-Cook, *Response Surface Methodology: Process and Product Optimization Using Designed Experiments*, Wiley, (2009).
 [9] B.T. Lin, M.D. Jean, J.H. Chou, *Appl. Surf. Sci.*, 253 (2007), 3254.
 [10] M. Masmoudi, D. Capek, R. Abdelhedi, F. El Halouani, M. Wery, *Surf. Coat. Technol.*, 200 (2006), 6651.
 [11] D.S. Correia, C.V. Gonçalves, S.S. Da Cunha Jr, V.A. Ferraresi, *J. Mater. Process. Technol.*, 160 (2005), 70.
 [12] J.S. Thella, R. Venugopal, *Powder Technol.*, 211 (2011), 54.
 [13] J. Feroso, M.V. Gil, B. Arias, M.G. Plaza, C. Pevida, J.J. Pis, F. Rubiera, *International Journal of Hydrogen Energy*, 35 (2010), 1191.
 [14] L. Dai, J. Peng, H. Zhu, *2nd International Symposium on High-Temperature Metallurgical Processing*, John Wiley & Sons, Inc., (2011), 101.
 [15] S. Mookherjee, A. Mukherjee, B.K. Dhindaw, H.S. Ray, *Trans. Inst. JPN.*, 26 (1986) 101..
 [16] X. Zhang, R. Wang, X. Yang, J. Yu, *Chemom. Intell. Lab. Syst.*, 89 (2007), 45.
 [17] O. Kubaschewski, C.B. Alcock, P.J. Spencer, *Materials thermochemistry*, 6, illustrated ed., Pergamon Press, (1993), 373.
 [18] G.S. Liu, V. Strezov, J.A. Lucas, L.J. Wibberley, *Thermochim. Acta*, 410 (2004) 133-140.
 [19] C.E. Seaton, J.S. Foster, J. Velasco, *Trans. Inst. JPN.*, 23 (1983), 490.
 [20] S. Halder, R.J. Fruehan, *Metall. Mater. Trans. B*, 39 (2008), 796.
 [21] T. Wiltowski, K. Piotrowski, H. Lorethova, L. Stonawski, K. Mondal, S.B. Lalvani, *Chem. Eng. Process.*, 44 (2005), 775.
 [22] I. Sohn, R.J. Fruehan, *Metall. Mater. Trans. B*, 36B (2005), 605.